Talanta 108 (2013) 59–65

Contents lists available at SciVerse ScienceDirect

Talanta

journal homepage: www.elsevier.com/locate/talanta

Development of multicolor carbon nanoparticles for cell imaging

Huiping Yan [a,b], Mingqian Tan [b,*], Demeng Zhang [b], Fansheng Cheng [c], Hao Wu [b], Meikun Fan [c], Xiaojun Ma [b], Jihui Wang [a,1]

[a] School of Food Science & Technology, Dalian Polytechnic University, Dalian 116034, PR China
[b] Laboratory of Biomedical Material Engineering, Dalian Institute of Chemical Physics, Chinese Academy of Sciences, Dalian 116023, PR China
[c] Chengdu Green Energy and Green Manufacturing Technology R&D Center, Chengdu 610207, PR China

ARTICLE INFO

Article history:
Received 28 December 2012
Received in revised form
25 February 2013
Accepted 27 February 2013
Available online 7 March 2013

Keywords:
Multicolor carbon nanoparticles
Fluorescence
Cell labeling

ABSTRACT

Multicolor carbon nanoparticles (CNPs) were prepared, characterized and developed as fluorescent probes for cell imaging. The fluorescent CNPs were prepared with a facile hydrothermal oxidation route by using linear polysaccharide cellulose and cyclic oligosaccharide cyclodextrin as carbon sources. The characterizations by transmission electron microscopy show that the prepared cellulose-CNPs and cyclodextrin-CNPs are spherical, well-dispersed in water with average diameters of 100 nm and 76 nm, respectively. Under the excitation of UV light, the CNPs are strongly luminescent with an excitation-dependent emission behavior and bathochromic emission properties. The fluorometric methods show that the cellulose-CNPs and cyclodextrin-CNPs are strongly fluorescent with fluorescence quantum yield of 7.47% and 4.49%, respectively. The multicolor CNPs have excellent photostability toward photobleaching. Strong near-infrared fluorescence of the carbon nanoparticles was observed with a 632.8 nm excitation wavelength laser. The oxidative metal ions like Hg(II), Cu(II) and Fe(III) show an quench effect on the fluorescence intensity of the CNPs. The multicolor CNPs were successfully used as fluorescent probes for mouse melanoma cells imaging. The results indicate that the multicolor CNPs derived from cellulose and cyclodextrin may have a great potential for the applications in bioimaging.

1. Introduction

Fluorescent semiconductor quantum dots (QDs) have been extensively used in biological applications, such as bio-molecular labeling, contrast agents, bio-sensing and drug delivery.[1–3] However, potential toxicity from heavy metals has drawn great attention on serious safety concern and environmental risks.[4,5] For this reason, various fluorescent nanoparticles made from alternatives materials with similar optical properties have been investigated as candidates for potential applications in optical imaging.[6–8] For example, we developed a method to prepare the lanthanide chelate-doped silica nanoparticles for highly sensitive time-resolved immunoassay[9–11]. The use of silica-doped fluorescent nanoparticles can improve the photostability and detection sensitivity of the nanoparticles. However, tedious synthesis steps and surface activation procedure of the nanoparticles were required for their use in bio-molecule labeling and cell imaging[9].

Carbon-based nanomaterials like carbon nanotubes, fullerenes, nanofibers and graphene nanosheets have been drawn great attention for their applications in nanosensors, electrical devices, catalysis reactors, drug delivery and electrochemistry.[12,13] Recent studies have shown that a new class of carbon nanoparticles (CNPs) exhibit promising fluorescent properties, such as high photostability, tuneable excitation and emission wavelength, low toxicity, good biocompatibility and bright electroluminescence.[14–18] The major element of CNPs, carbon, is hardly considered as a toxic substance compared with the heavy metals from conventional QDs. Because of these features, various methods for fluorescent CNP synthesis have been reported by using carbon-based materials as carbon resources.[14,19,20] For example, top-down methods include laser ablation of carbon powder[14], electrochemical oxidation[21] and arc discharge[22]; bottom-up methods consist of microwave synthesis,[23,24] combustion soots of candles,[25,26] thermal oxidation of carbon precursor by employing silica or zeolites as carriers[27,28] commercial activated carbon[29], lampblack[30] and watermelon peel as carbon resources[31]. All these methods suffer to some degree from drawbacks like tedious processes, harsh synthetic conditions or expensive starting materials. Preparation of fluorescent CNPs from bioprecursors may provide a new approach for bottom-up CNPs fabrications. Although carbon nanoparticles derived from

* Corresponding author. Tel.: +86 411 84379139; fax: +86 411 84379096.
E-mail addresses: mqtan@yahoo.cn (M. Tan), wangjh@dlpu.edu.cn (J. Wang).
[1] Tel./fax: +86 411 86323018.

0039-9140/$ - see front matter © 2013 Elsevier B.V. All rights reserved.
http://dx.doi.org/10.1016/j.talanta.2013.02.074

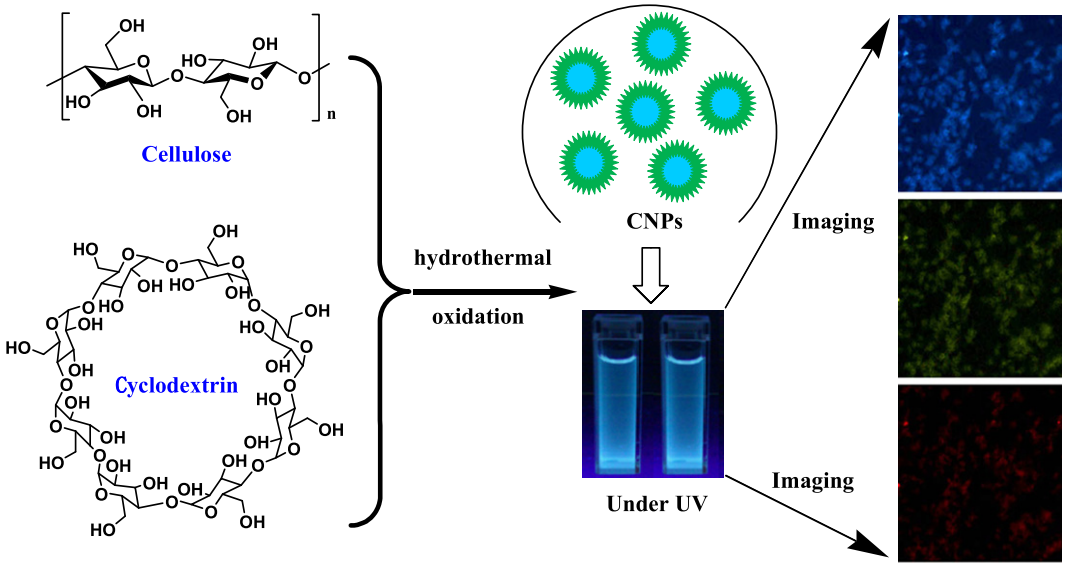

Scheme 1. Preparation scheme of multicolor CNPs from cellulose and cyclodextrin. (For interpretation of the references to color in this scheme legend, the reader is referred to the web version of this article.)

glucose and sucrose have been reported, [20,32] to the best of our knowledge, the direct synthesis of fluorescent CNPs from linear polysaccharides and cyclic oligosaccharides and their fluorescent properties remains less studied.

Herein, we report a one-step method of alkali-assisted hydrothermal oxidation of polysaccharide cellulose and cyclic oligosaccharide cyclodextrin, to prepare multicolor fluorescent CNPs (Scheme 1). The CNPs that were obtained emit bright and colorful fluorescence covering the whole visible spectral range. The multicolor CNPs are highly water-soluble, nano-sized (100 nm, 76 nm) and quite stable against photo-bleaching as compared with conventional organic dyes. Strong near infrared fluorescence of the CNPs was detected using a 632.8 nm laser as excitation source. The oxidative metal ions like Hg(II), Cu(II) and Fe(III) displayed an quench effect on the fluorescence intensity of the CNPs. The multicolor CNPs were successfully used as fluorescent probes for mouse melanoma cells imaging. The developed multicolor CNPs derived from saccharides may have a potential for the applications in biomedical fields.

2. Experimental

2.1. Materials and instrumentation

Cellulose was purchased from Fluka (Avicel PH-101) and cyclodextrin was purchased from Chemical Reagent Co. Ltd. (Tianjin, China). Dialysis bag was purchased from Genestar Biotechnology Co. Ltd. (Shanghai, China). Mouse melanoma cell line B16-F10 was purchased from KeyGen Biotechnology Co. Ltd. (Nanjing, China).

A JEOL model JEM-2000EX transmission electron microscope was used for measuring the shape and size of the nanoparticles. UV–vis absorption spectra were measured on a Shimadzu UV2550 UV–vis spectrophotometer. Fourier transform infrared spectra were performed using a VECTOR 22 FTIR spectrometer with a KBr pellets. Fluorescence spectra and emission lifetime were measured on a Perkin–Elmer LS 55 spectrofluorometer. Zeta potential was determined by laser Doppler velocimetry at 25 °C using a Nano ZS90 Zetasizer (Malvern Instruments, Malvern, U.K.). NIR emission spectra were measured by Princeton Instrument Acton SP2500 Spectrograph with a PIXIS 100 CCD equipped with a 632.8 nm He-Ne laser (model, 25 LHP 928-230; power, 25 mW) as an excitation source. The integration time for cellulose-CNPs and cyclodextrin-CNPs are 1 ms and 500 ms, respectively. Fluorescence imaging measurements of cell labeling were performed on a inverted Nikon Te-2000 U microscope with an excitation filter of 330–380 nm, 450–490 nm and 510–560 nm for blue, green and red color respectively. *Ex vivo* imaging was carried out with a CRi Meastro Ex *in vivo* imaging system (Caliper Life Sciences Inc. U.S.A.).

2.2. Preparation of carbon nanoparticles (CNPs)

Multicolor CNPs were synthesized directly from alkali-assisted hydrothermal oxidation of cellulose or cyclodextrin aqueous solution according to a modified procedure as previously described. [32] Briefly, 2.0 g of cellulose or cyclodextrin and 0.2 g of sodium hydroxide were added to 30 ml of water with vigorous stirring. The mixture solution was then sealed into a Teflon-lined stainless-steel autoclave and heated at a constant temperature of 160 °C for 4 hours. Then, the solution was cooled at room temperature and the dark brown solution was obtained. The multicolor CNPs were isolated by centrifuge at a speed of 10000 rpm for 20 min to remove the deposit. The resulting CNPs were neutralized by 1 mol/L hydrochloric acid solution and extensively dialyzed against distilled water through a dialysis membrane with a molecular weight cutoff of 3000 to remove the impurities. The multicolor CNPs were purified with Sephadex G25 column and dried in a lyophilizer for the following use.

2.3. Metal ions effects on fluorescence intensity

Standard aqueous solutions (10^{-4} mol/L or 10^{-6} mol/L) of $CaCl_2$, $MgCl_2 \cdot 6H_2O$, $CuSO_4 \cdot 5H_2O$, NaCl, K_2CO_3, $ZnCl_2$, $NiSO_4$ $6H_2O$, $FeCl_3$, Hg_2Cl_2 and $CdCl_2$ were prepared in distilled water. To 4.5 ml of standard metal ions solution was added 0.5 ml of the multicolor CNPs solution (0.5 mg/ml) and the mixture was stirred at room temperature. The fluorescent intensity of mixed solution was measured with LS55 fluorescence spectrofluorometer (Perkin–Elmer) at the wavelength of 450 nm. The fluorescence intensity of the luminescent materials was normalized and plotted as the mean values of three measurements ± SD (standard deviation).

2.4. Photo-stability experiment

The photostability experiment of the multicolor CNPs, rhodamine B and fluorescein in distilled water against photo-bleaching was performed under a 40 W incandescent lamp as an excitation source. The multicolor CNPs, rhodamine B or fluorescein were added to a 10 mm fluorescence cuvette and kept 10 cm away from the excitation lamp. The fluorescence intensity of the multicolor CNPs was measured with spectrofluorometer every 10 min.

2.5. Mouse melanoma cell imaging

Mouse melanoma cells (B16-F10) cultured in 5 mL of RPMI-1640 medium with 10% Fetal Bovine Serum or FBS in culture flask were trypsinized and seeded in 24-well tissue culture plates with a glass slide at the bottom at 3×10^4 cells/well at 37 °C. To each well was added 100 μL fluorescent CNPs (3.8 mg/mL) and 400 μL medium. After 5 h incubation, the glass covered with cells was washed thoroughly with PBS buffer and the cells were fixed with formalin. Cell-imaging was performed under an inverted Nikon TE-2000 U fluorescent microscope and the fluorescence images were collected in blue, green and red region. Exposure time was 300 ms.

3. Results and discussion

3.1. Preparation of nanoparticles

Hydrothermal oxidation method is one of the easy and efficient methods for the preparation of fluorescent CNPs. Generally, carbon source of cellulose or cyclodextrin undergo only one-step alkali-assisted hydrothermal oxidation to form the multicolor fluorescent CNPs. These two kinds of saccharides were selected as carbon sources for fluorescent CNPs preparation because 1) cellulose is a linear polysaccharide polymer[33] with many glucose monosaccharide units which is one of three common and principal types of polysaccharides (cellulose, starch and glycogen) and 2) cyclodextrin is a cyclic oligosaccharide resulting from the cyclomaltodextrin glucanotransferase catalyzed degradation of starch[34]. No report has been found in the literature in which the linear polysaccharide and cyclic oligosaccharide have been used for multicolor CNPs preparation. The development of multicolor CNPs derived from cellulose or cyclodextrin might provide new candidates for the application of bio-imaging.

Our results showed that the cellulose and cyclodextrin were easily etched into individual CNPs by treatment with inorganic alkali at a mild temperature (160 °C). The mechanism for the formation of multicolor CNPs involves hydrothermal carbonization of the major constituents of sugars. The resulting multicolor CNPs are strongly luminescent under the excitation of ultra-violet (UV) light (Scheme 1). As shown in Fig. 1, the cellulose-CNPs and cyclodextrin-CNPs prepared by this method are spherical and well-dispersed. The average particle sizes of cellulose-CNPs and cyclodextrin-CNPs are about 100 nm and 76 nm, respectively (Table 1). The size distribution histograms suggest that the particle size of cellulose-CNPs and cyclodextrin-CNPs are in the range of 85–123 nm and 62–92 nm, respectively. The cellulose is composed of a long chain of hundreds of glucose units. The molecular weight of cellulose is much larger than that of the cyclodextrin. The different sizes and size distributions of the CNPs might be ascribed to the different molecular weight of the starting materials.

3.2. Fluorescence characterization of CNPs

The UV–vis and fluorescence spectra of the multicolor CNPs in water are shown in Fig. 2. The multicolor CNPs exhibit UV–vis absorption from 200 nm to 500 nm, showing a maximum peak at 259 nm and 295 nm for cellulose-CNPs and cyclodextrin-CNPs, respectively. The CNPs aqueous solution is yellowish, transparent and clear under daylight. The colored spectra and insert plots in Fig. 2 show the fluorescence spectra of the multicolor CNPs under the excitation of different excitation wavelengths. The CNPs exhibit an excitation-dependent emission phenomenon. With the increasement of excitation wavelength, the CNPs emit at longer wavelength, showing similar luminescent property with the CNPs from glucose and sucrose. The bathochromic emission of the CNPs has been extensively reported previously.[14,15,20,28] The emission intensity shows the highest valve of 439 nm and 405 nm for cellulose-CNPs (FWHM, 90 nm) and cyclodextrin-CNPs (FWHM, 135 nm), respectively, under the excitation at 360 nm. It is reasonable to assume that the different carbon resources lead to the different excitation energy traps and the different fluorescence properties. The quantum confinement of the multicolor CNPs surface energy trap is thought to be the reason for the strong emission. In fact, the exact mechanism of the CNPs' photoluminescence is currently not completely clear and further efforts are needed to reveal the phenomenon.

Interestingly, we also observed near-infrared (NIR) emission of the fluorescent CNPs when the samples were excited with a 632.8 nm laser (Fig. 3). The maximum emission peaks for

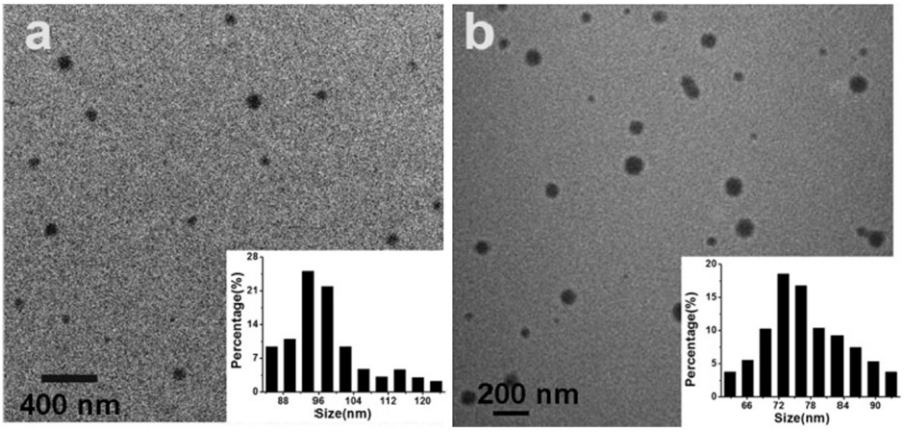

Fig. 1. TEM images of fluorescent CNPs prepared from cellulose (a) and cyclodextrin (b). The inset histograms are the size distributions of CNPs measured by TEM.

Table 1
Physicochemical parameters of the CNPs.

Sample	Excitation wavelength (nm)									λ_{Abs} (nm)	Size (nm)	FWHM (nm)	Zeta potential (eV)	QY (Φ, %)
	300	320	340	360	380	400	420	440	460					
Cel-CNPs	*433*	*434*	*445*	*438*	*458*	*490*	*510*	*532*	*540*	260	100	90	−19.4	7.47
Cyc-CNPs	*383*	*380*	*386*	*407*	*420*	*424*	*461*	*502*	*536*	294	76	135	−19.8	4.49

Excitation wavelengths are from 300 nm to 460 nm in 20 nm increments, data of italics show corresponding emission wavelength (nm); FWHM, the full width at a half maximum; QY, Quantum yield at 360 nm.

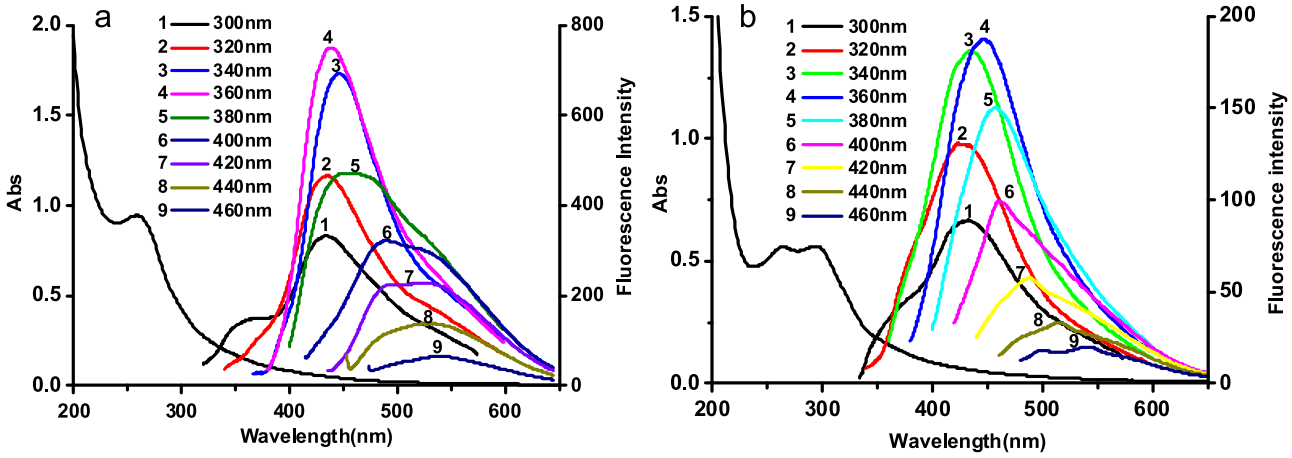

Fig. 2. UV/Vis absorption (Abs) and fluorescence emission spectra of CNPs prepared from cellulose (a) and cyclodextrin (b) in water. Excitation wavelengths are from 300 nm to 460 nm in 20 nm increments.

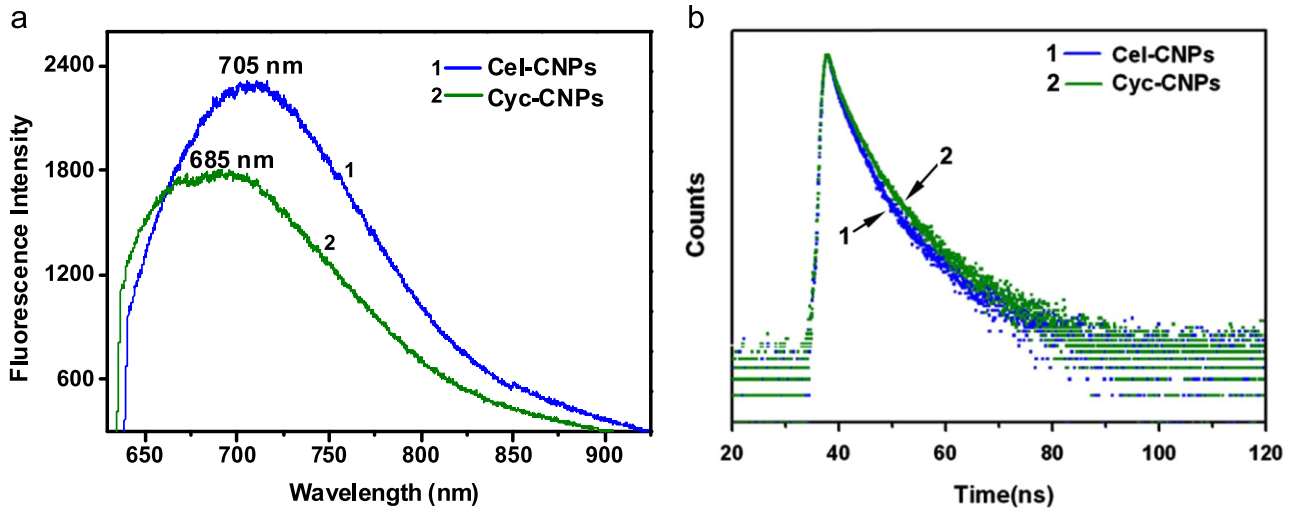

Fig. 3. Near infrared fluorescence spectra of CNPs excited with a helium-neon laser at wavelength of 632.8 nm (a). (b) Fluorescence decay curves of Cel-CNPs (λ_{ex}=375 nm,.λ_{em}=456 nm) and Cel-CNPs (λ_{ex}=375 nm,.λ_{em}=450 nm).

cellulose-CNPs and cyclodextrin-CNPs are 705 nm and 685 nm, respectively. The NIR emission of CNPs is an attracting feature that has been reported from sucrose and starch derived CNPs.[32] It should be noted that NIR emissions of the prepared CNPs excited by NIR excitation (632.8 nm) are particularly significant and useful for deep tissue optical imaging. The NIR emissive CNPs might offer great potential for *in vivo* optical imaging and related biomedical applications.

The fluorescence quantum yields (QY) of the cellulose-CNPs and cyclodextrin-CNPs were measured to be 7.47% and 4.49%, (the experimental uncertainty < 15%) respectively (Table 1) by using a reported method[29] calculated using the equation of $\phi_1 = I_1 A_2 \phi_2 / I_2 A_1$ with a standard QY of ϕ_2=10.0% for quinine sulfate at 350 nm in 0.1 M H_2SO_4. In the equation, I_1 and I_2 are the fluorescence intensities of the nanoparticles and the standard, and A_1 and A_2 are the optical densities of the nanoparticles and the standard, respectively. The quantum yield gives the probability of the excited state being deactivated by fluorescence rather than by another non-radiative mechanism. When the CNPs absorb a photon of light, an energetically excited state is formed.

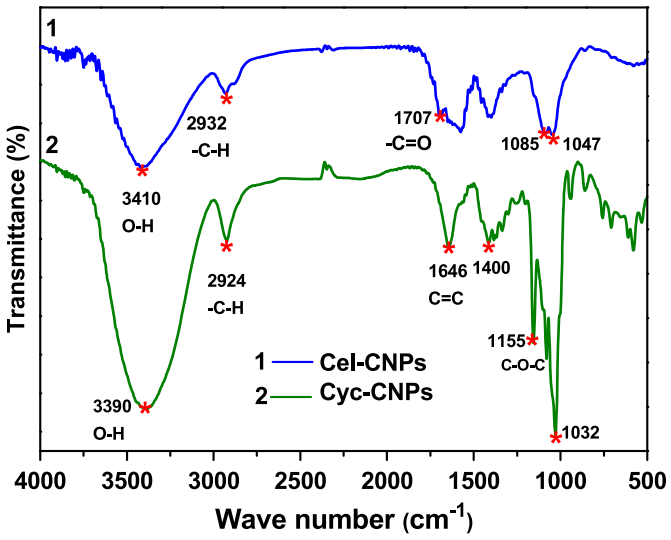

Fig. 4. FT-IR spectra of cellulose-CNPs and cyclodextrin-CNPs.

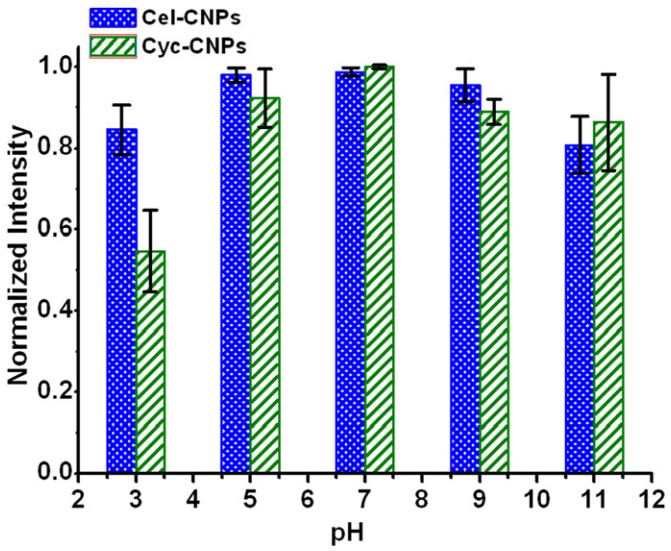

Fig. 5. pH effects on the fluorescence of cellulose-CNPs and cyclodextrin-CNPs at 360 nm (The number of points for the error bars is 6).

The fate of these activated CNPs is varied, depending upon the exact nature of the CNPs. Thus, it is not surprising that the cyclodextrin-CNPs with a smaller particle size range (higher surface area) have a smaller quantum yield. Similar results were also reported in the previous work.[29] The QY of cellulose-CNPs is higher than that of cyclodextrin-CNPs indicating that cellulose-CNPs have better efficiency of the fluorescence process. These QY values are comparable to those of the carbon dots derived from candle soot, active carbon[25] and greater than those of the CNPs from glucose and sucrose[32], indicating that the QY of the CNPs should be high enough for bio-imaging applications.

3.3. FT-IR characterization of CNPs

FT-IR spectra in Fig. 4 show broad and intense peaks around 3410 cm^{-1} correspond to the O–H stretching vibration, indicating the existence of large numbers of hydroxyl groups. The peaks at around 1646 cm^{-1} are attributed to carboxyl groups and aromatic C=C vibrations. Another broad peak with increased intensity at 1400 cm^{-1} indicates the existence of C–H bonds, while the strongest peak between1200–1000 cm^{-1} is due to the C–O stretching vibration. The existence of carboxyl groups offers good water solubility and the carboxylic groups on the multicolor CNPs surface provide potential platform for various surface modification. The zeta-potential measurement revealed that both CNPs had negative values less than 18 mV at pH 6.5, indicating the existence of carboxyl groups. This provided further evidence in supporting the FT-IR analysis.

4. pH and photo stability experiments of CNPs

The pH value of the solution affects the fluorescence intensity of the multicolor CNPs (Fig. 5). Similar to the previous report,[19] the fluorescence intensity is relatively stable at physiogical pH for both CNPs, while the fluorescence intensity decreases significantly (by 55–81%) upon changing from a neutral to either an acidic or a basic solution (at pH 3 or 11). The pH-sensitive property of the multicolor CNPs could be explored for tumor imaging.[35] Additionally, as shown in the Fig. 6, the multicolor CNPs showed excellent photostability as compared with conventional organic dyes, fluorescein and rhodamine B. The fluorescence intensity of CNPs remained unchanged even after being irradiated with a 40 W incandescent lamp for 50 min, whereas

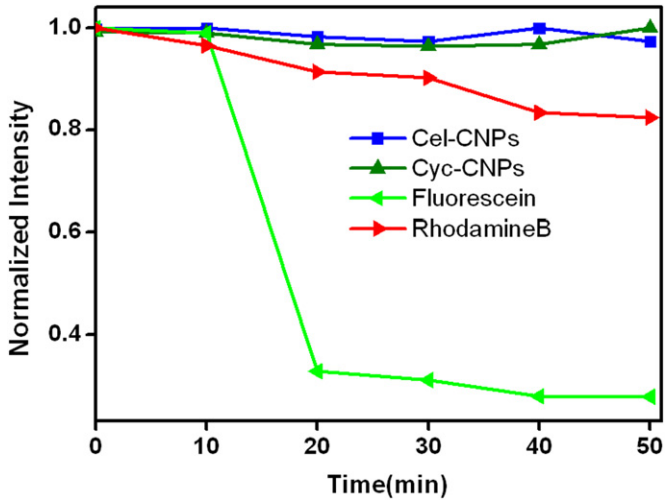

Fig. 6. Photostability of cellulose-CNPs, cyclodextrin-CNPs, fluorescein and RhodamineB.

the emission intensity of rhodamine B and fluorescein decreased 18% and 73% respectively at the same period. The excellent photostability of the CNPs is essential for the use as fluorescent probes in biological analysis[29].

4.1. Metal ions effects on fluorescence intensity

Metal ions effects on emission intensity of both multicolor CNPs were investigated. As shown in Fig. 7, 100 μM aqueous solutions of Hg(II), Cu(II), and Fe(III) ions provoked a decrease of 20%–60% in the fluorescence intensity of multicolor CNPs while the equal amount of the ions Ni(II), Na(I), K(I), Zn(II), Ca(II), Mg(II) and Cd(II) showed no measurable quenching effect on the fluorescence of the CNPs. In particularly, Fe(III) exerted a substantial effect on the multicolor CNPs low to 40% for cellulose-CNPs. No obviously different effects from metal ions on fluorescence intensity between cellulose-CNP and cyclodextrin-CNP were found. As we know, Hg(II), Cu(II), and Fe(III) ions are a class of oxidant which can quench the fluorescence of CNPs due to facilitating non-radiative electron/hole recombination annihilation through an effective electron transfer process.[36]

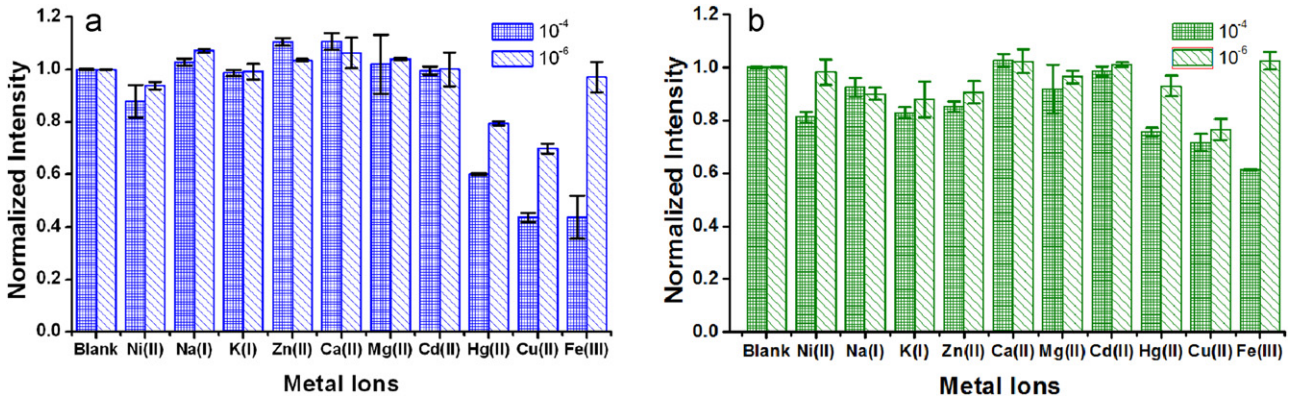

Fig. 7. Metal effects on fluorescence intensity of cellulose-CNPs (a) and cyclodextrin-CNPs (b). (The number of points for the error bars is 6).

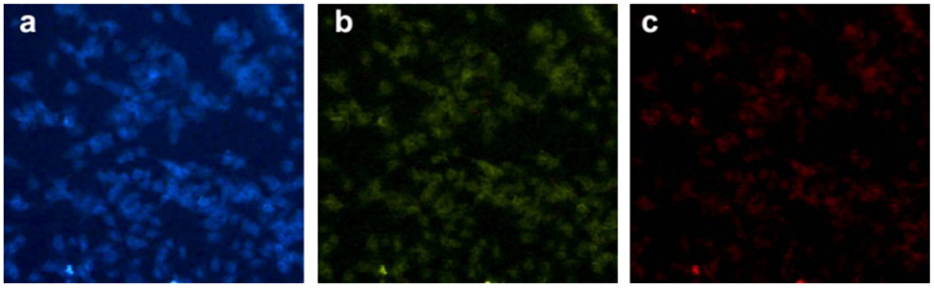

Fig. 8. Fluorescence images of mouse melanoma cells incubated with cellulose-CNPs for 5 h. The images were obtained with an inverted Nikon TE-2000 U microscope with an excitation filter of 330–380 nm (a), 450–490 nm (b) and 510–560 nm (c). Exposure time was 300 ms.

The quenching effects of these metal ions on multicolor CNPs emission could be explored for the development of smart sensor in nanotechnology and nano-devices [37].

4.2. Mouse melanoma cell labeling

Cell imaging technique is valuable in defining cell behaviors that are necessary for invasion, intravasation, and extravasation. These features make cell imaging a requisite technique for addressing questions in cell biology, cancer research and developmental biology. The possibility of the multicolor CNPs as probes for cell imaging was explored. We have performed *in vitro* cellular uptake experiment in mouse melanoma cells (B16-F10). We chose mouse melanoma cells for CNPs imaging because melanoma is much more dangerous which cause the majority of deaths related to skin cancer. These cells (B16-F10) are more metastatic than B16F1. Since imaging tumor cell lines utilizing fluorescence techniques is gaining increasing attention, it is of paramount importance to incorporate multicolor CNPs to these cells. After the tumor cells were incubated with cellulose-CNPs for 5 h at 37 °C, the fluorescence images of CNP-treated cells in Fig. 8 clearly showed that the multicolor CNPs were able to label the cells. Moreover, blue, green and red color images could be obtained because of the excitation dependent fluorescence feature of the multicolor CNPs. This value was essential for identifying the CNPs and other fluorescent probes in multiple cell-labeling. Unlike the CNPs prepared from candle soot, the fluorescent intensity of the CNPs was independent on pH in the physiological and pathological pH range of 5–9.[25] All these features demonstrate that the multicolor CNPs derived from cellulose and cyclodextrin have very good biocompatibility and make them good candidates for cell imaging. Although the imaging of the cancer cells using these CNPs did not exhibit selection over normal cells, if the CNPs were conjugated with melanoma specific targeting moieties, we believe that the tumor specific CNPs may have a potential for melanoma selective imaging. Design and structural optimization of the targeted multicolor CNPs will be performed in the future studies to improve its tumor specificity and binding affinity.

5. Conclusion

In summary, novel multicolor CNPs derived from cellulose and cyclodextrin were developed, characterized and used for mouse melanoma cells imaging. As new fluorescent probes, the advantages of the multicolor CNPs include highly water solubility, strong luminescence, good stability in physiological pH range and excellent inertness against photo-bleaching, make them good candidates as probes for the applications of bio-imaging. The results of melanoma cells imaging show that the developed multicolor CNPs are effective for imaging analysis of cells. It can be expected that the new multicolor CNPs would be widely useful for bio-molecule imaging analysis, such as tissue imaging, protein fluorescence bio-imaging technology, and other biomedical or biotechnology applications.

Acknowledgments

This work was supported by the National Nature Science Foundation of PR China (Grant No. 91227126) and the Dalian Institute of Chemical Physics (DICP)-100-talents Program Foundation of Chinese Academy of Sciences.

References

[1] A. Alivisatos, Science 271 (1996) 933–937.
[2] X. Gao, Y. Cui, R. Levenson, L. Chung, S. Nie, Nat. Biotechnol. 22 (2004) 969–976.
[3] X. Michalet, F. Pinaud, L. Bentolila, J. Tsay, S. Doose, J. Li, G. Sundaresan, A. Wu, S. Gambhir, S. Weiss, Science 307 (2005) 538–544.
[4] P. Lin, J.W. Chen, L.W. Chang, J.P. Wu, L. Redding, H. Chang, T.K. Yeh, C.S. Yang, M.H. Tsai, H.J. Wang, Y.C. Kuo, R.S.H. Yang, Environ. Sci. Technol. 42 (2008) 6264–6270.
[5] R. Hardman, Environ. Health Perspectives 114 (2006) 165–172.
[6] S. Kalem, P. Werner, V. Talalaev, M. Becker, O. Arthursson, N. Zakharov, Nanotechnology 21 (2010).
[7] T.J. Boyle, L.A.M. Ottley, A. Velasquez, B.A. Dimos, Abstr. Pap. Am. Chem. S 241 (2011).
[8] D.J. Zhang, X.M. Wang, Z.A. Qiao, D.H. Tang, Y.L. Liu, Q.S. Huo, J. Phys. Chem. C 114 (2010) 12505–12510.
[9] M.Q. Tan, Z.Q. Ye, G.L. Wang, J.L. Yuan, Chem. Mater. 16 (2004) 2494–2498.
[10] Z.Q. Ye, M.Q. Tan, G.L. Wang, J.L. Yuan, J. Mater. Chem. 14 (2004) 851–856.
[11] Z.Q. Ye, M.Q. Tan, G.L. Wang, J.L. Yuan, Talanta 65 (2005) 206–210.
[12] Y.A. Kim, T. Hayashi, M. Terrones, M. Endo, M.S. Dresselhaus, J. Biomed. Nanotechnol. 2 (2006) 106–108.
[13] Y. Xu, L. Yang, P.G. He, Y.Z. Fang, J. Biomed. Nanotechnol. 1 (2005) 202–207.
[14] Y.P. Sun, B. Zhou, Y. Lin, W. Wang, K.A.S. Fernando, P. Pathak, M.J. Meziani, B.A. Harruff, X. Wang, H.F. Wang, P.J.G. Luo, H. Yang, M.E. Kose, B.L. Chen, L.M. Veca, S.Y. Xie, J. Am. Chem. Soc. 128 (2006) 7756–7757.
[15] L. Cao, X. Wang, M.J. Meziani, F.S. Lu, H.F. Wang, P.J.G. Luo, Y. Lin, B.A. Harruff, L.M. Veca, D. Murray, S.Y. Xie, Y.P. Sun, J. Am. Chem. Soc. 129 (2007) 11318–11319.
[16] S.T. Yang, X. Wang, H.F. Wang, F.S. Lu, P.J.G. Luo, L. Cao, M.J. Meziani, J.H. Liu, Y.F. Liu, M. Chen, Y.P. Huang, Y.P. Sun, J. Phys. Chem. C 113 (2009) 18110–18114.
[17] F. Wang, Y.H. Chen, C.Y. Liu, D.G. Ma, Chem. Commun. 47 (2011) 3502–3504.
[18] I.L. Christensen, Y.P. Sun, P. Juzenas, J. Biomed. Nanotechnol. 7 (2011) 667–676.
[19] X.H. Wang, K.G. Qu, B.L. Xu, J.S. Ren, X.G. Qu, J. Mater. Chem. 21 (2011) 2445–2450.
[20] Y.H. Yang, J.H. Cui, M.T. Zheng, C.F. Hu, S.Z. Tan, Y. Xiao, Q. Yang, Y.L. Liu, Chem. Commun. 48 (2012) 380–382.
[21] Q.L. Zhao, Z.L. Zhang, B.H. Huang, J. Peng, M. Zhang, D.W. Pang, Chem. Commun. (2008) 5116–5118.
[22] X.Y. Xu, R. Ray, Y.L. Gu, H.J. Ploehn, L. Gearheart, K. Raker, W.A. Scrivens, J. Am. Chem. Soc. 126 (2004) 12736–12737.
[23] S. Chandra, P. Das, S. Bag, D. Laha, P. Pramanik, Nanoscale 3 (2011) 1533–1540.
[24] H. Zhu, X.L. Wang, Y.L. Li, Z.J. Wang, F. Yang, X.R. Yang, Chem. Commun. (2009) 5118–5120.
[25] H.P. Liu, T. Ye, C.D. Mao, Angew. Chem. Int. Ed. 46 (2007) 6473–6475.
[26] S.C. Ray, A. Saha, N.R. Jana, R. Sarkar, J. Phys. Chem. C 113 (2009) 18546–18551.
[27] R.L. Liu, D.Q. Wu, S.H. Liu, K. Koynov, W. Knoll, Q. Li, Angew. Chem. Int. Ed. 48 (2009) 4598–4601.
[28] A.B. Bourlinos, A. Stassinopoulos, D. Anglos, R. Zboril, V. Georgakilas, E.P. Giannelis, Chem. Mater. 20 (2008) 4539–4541.
[29] Z.A. Qiao, Y.F. Wang, Y. Gao, H.W. Li, T.Y. Dai, Y.L. Liu, Q.S. Huo, Chem. Commun. 46 (2010) 8812–8814.
[30] X.-J. Mao, H.-Z. Zheng, Y.-J. Long, J. Du, J.-Y. Hao, L.-L. Wang, D.-B. Zhou, Spectrochim Acta Part A 75 (2010) 553–557.
[31] J.J. Zhou, Z.H. Sheng, H.Y. Han, M.Q. Zou, C.X. Li, Mater. Lett. 66 (2012) 222–224.
[32] X.D. He, H.T. Li, Y. Liu, H. Huang, Z.H. Kang, S.T. Lee, Colloid Surf. B 87 (2011) 326–332.
[33] E. Zablackis, J. Huang, B. Muller, A.G. Darvill, P. Albersheim, Plant Physiol. 107 (1995) 1129–1138.
[34] C.B. Lebrilla, Acc. Chem. Res. 34 (2001) 653–661.
[35] H. Koo, M.S. Huh, I.C. Sun, S.H. Yuk, K. Choi, K. Kim, I.C. Kwon, Acc. Chem. Res. 44 (2011) 1018–1028.
[36] Y.S. Xia, C.Q. Zhu, Talanta 75 (2008) 215–221.
[37] L. Zhou, Y.H. Lin, Z.Z. Huang, J.S. Ren, X.G. Qu, Chem. Commun. 48 (2012) 1147–1149.